Available online at www.sciencedirect.com
SCIENCE DIRECT
Polymer 46 (2005) 8745–8751
polymer
www.elsevier.com/locate/polymer

Copolymer crystallization: Approaching equilibrium

Buckley Crist*, Terry M. Finerman[1]

Department of Materials Science and Engineering, Northwestern University, Evanston, IL 60208-3108, USA

Received 29 November 2004; received in revised form 8 March 2005; accepted 11 March 2005
Available online 19 July 2005

Abstract

Melt crystallization of random copolymers leads to solids with crystalline fraction w_c and final melting temperature T_m^f that are substantially below the predictions of Flory's equilibrium crystallization theory. Model ethylene/butene random copolymers, when crystallized as multilayer films by rapid solvent evaporation, exhibit increased w_c (50% relative) and T_m^f (4 K) compared to melt crystallized values. For a copolymer with 0.92 mol fraction ethylene, the density-derived crystallinity $w_c = 0.6$ is the same as that from Flory's theory, although the maximum observable crystal thickness from T_m^f remains about 25% of the theory value. These effects are seen because crystallization from solution occurs without many of the constraints to segment dynamics that limit crystalline fraction during melt crystallization. Crystal thickness is dominated by secondary nucleation barriers in both melt and solution. Chain or sequence folding is much more regular in the solution crystallized material, and amorphous layer thickness is reduced from about 8 nm to 3 nm.

Keywords: Crystallization; Copolymer; Thermodynamic

1. Introduction

It is well known that copolymerization reduces the crystalline fraction, reduces the melting temperature and broadens the melting range of a crystallizable polymer. These features are all captured qualitatively by Flory's equilibrium theory of copolymer crystallization [1], but experimental crystallinity and melting temperature are invariably lower than those predicted by theory. Fig. 1 depicts the essence of Flory's approach. Statistical copolymer chains are composed of crystallizable segments of different lengths that are terminated by non-crystallizable comonomer units. When the molten or dissolved polymer is cooled, the longest sequences associate first to form extended sequence crystals. Further cooling results in the similar crystallization of shorter sequences, etc. and the non-crystalline fraction is composed primarily of comonomer plus those sequences too short to form stable crystals at the temperature T. An additional small amorphous contribution comes from imperfect matching of sequence lengths as sketched. This thermodynamic model of crystallization is just the reverse of melting over a broad temperature range. With this in mind, Fig. 2 shows the Flory model in a manner analogous to a differential scanning calorimetry (DSC) curve. Here p is the sequence perpetuation probability, equal to the mole fraction of crystallizable monomer for a random copolymer, and the weight fraction crystallinity w_c is calculated with parameters for ethylene–butene copolymers [2]. Clearly evident is the shift of melting (or crystallization) to lower temperatures and a broadening of the transition range with smaller p (increased non-crystallizable comonomer). Vertical lines indicate melting temperatures. Those below the baseline give the equilibrium T_m^c of the two copolymers:

$$T_m^c = T_m^0 + \frac{R}{\Delta H_u} \ln p \tag{1}$$

Here T_m^0 is the equilibrium melting temperature of a perfect (infinite) polymer crystal, and ΔH_u is the heat of fusion per mole of repeat units (e.g. C_2H_4). What is generally not appreciated is that T_m^c is unobservable in an experiment, because the number of extended sequences of unbounded length that are predicted to melt at T_m^c is virtually zero. A more realistic measure of equilibrium melting is the final observable melting temperature T_m^f marked by the upper set

* Corresponding author. Fax: +1 847 491 7820.
E-mail address: b-crist@northwestern.edu (B. Crist).
[1] Present address: L&L Products, 159 McLean Drive, Romeo, MI 48065, USA.

0032-3861/$ - see front matter © 2005 Elsevier Ltd. All rights reserved.
doi:10.1016/j.polymer.2005.03.124

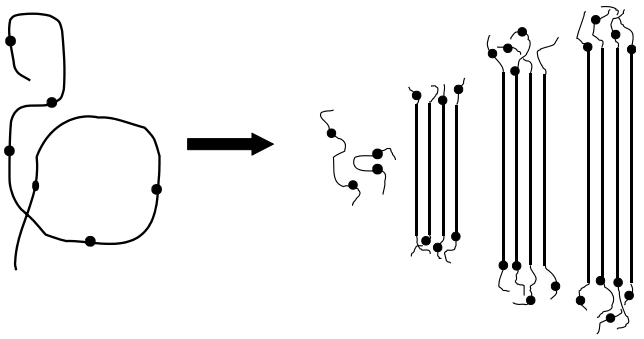

Fig. 1. Sketch of a representative copolymer chain in the melt or solution state and in the partially crystalline state considered by the Flory model. Non-crystallizable comonomer units are represented by black spheres, and light lines represent crystallizable sections that remain amorphous.

of lines in Fig. 2. At T_m^f the extended sequence crystals of length l_f are present in quantities large enough to be noticed when melting. In fact, this final melting temperature is given to an excellent approximation by the Gibbs–Thomson relation [3,4]:

$$T_m^f = T_m^c\left(1 - \frac{2\sigma v_u}{l_f \Delta H_u}\right) \tag{2}$$

As usual, it is assumed that the final crystals of thickness l_f that melt are plate-like (lamellar) with basal surface energy σ; v_u is the molar volume of a repeat unit. The quantities σ and ΔH_u are those for homopolymer crystals, because the last melting crystals in question are formed from long sequences that are essentially devoid of comonomer. While Eq. (2) is correct for the melting of equilibrium crystals, its predictive value for T_m^f is limited because there is no analytical method to obtain the crystal thickness l_f from copolymer composition.

Flory's model makes no allowance for constraints to the sorting of segments according to size, nor for nucleation

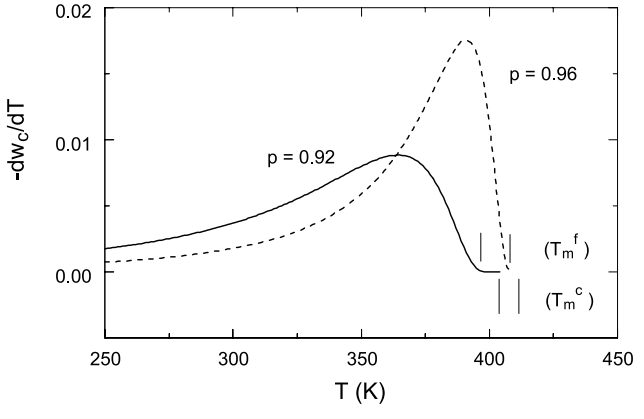

Fig. 2. The derivative of crystallinity-temperature curves calculated from the Flory theory for ethylene–butene copolymers. $-dw_c/dT$ is the change in weight fraction crystallinity w_c at a particular temperature; this format is directly comparable to a DSC curve. The parameter p (mole fraction of crystallizable monomer) corresponds to the two copolymers examined in this paper. Vertical lines represent the end of observable melting T_m^f and the unobservable thermodynamic limit T_m^c.

barriers that hinder the formation of extended segment crystals. Departures from equilibrium crystallization are clearly responsible for both crystalline fraction and melting range lying below the theoretical values. Indeed, Flory was among the earliest to acknowledge that the first-formed crystals create restraints to further crystallization at lower temperatures [5]. Other views have been expressed on this subject. Wunderlich, for instance, suggested that copolymer chains may crystallize with neighboring, randomly mixed sequence lengths that have no ability to sort themselves [6]. Killian, on the other hand, argues that equilibrium crystallization and melting occur with the aid of segment diffusion over small distances that are adequate to maintain equilibrium within 'microdomains' [7]. Regardless of constraints to the crystallizing fraction, melting temperatures that are below the equilibrium range are the unambiguous consequence of long sequences crystallizing in folded, not extended, conformations [8,9]. Extension of Eq. (2) to folded sequence, non-equilibrium crystals is straightforward. The useful result is that the maximum crystal thickness l_f in a crystallized copolymer can be established from the final melting temperature T_m^f. The reader should be reminded, however, that Eq. (2) is valid only for final melting when the composition of the melt is equal to the global copolymer composition. The relation between melting temperature and crystal thickness is altered (T_m is additionally depressed) when crystallization elevates the comonomer concentration in the melt.

We report here on model ethylene–butene random copolymers that are crystallized not only from the melt but also from solution as thin layers. Crystallinity from solution is seen to approach the theoretical equilibrium value, although the maximum melting temperature is still appreciably below its theoretical counterpart. Increased chain mobility in the solution state overcomes many of the impediments to sequence association, but crystal thickness remains limited by secondary nucleation barriers.

2. Experimental

Hydrogenated polybutadiene is a model random ethylene–butene random copolymer that is compositionally uniform and nearly monodisperse with respect to degree of polymerization [10]. HPB-20 has 20 ethyl branches per 1000 backbone C atoms and $M = 161$ kg/mol, and HPB-39 has 39 ethyl branches and $M = 171$ kg/mol; these materials were used in earlier studies [11]. For reference, the sequence perpetuation parameter p is 0.96 for HPB-20 and 0.92 for HPB-39, the same as in the calculated curves of Fig. 2. Polymers were dissolved in cyclohexane ($\sim$3 g/L) at 75 °C., from which aliquots of a few milliliters were pipetted into a 40 mm $\times$ 40 mm mold and the solvent evaporated with the aid of flowing room temperature air. The resulting semicrystalline film was $\sim$4 μm thick. This

process was repeated 30–50 times to build up a multilayer film of thickness ~0.2 mm.

The multilayer films (L) were vacuum dried at room temperature, then studied by density (gradient column) and DSC (Perkin–Elmer DSC-2 at 5 °C/min). X-ray diffraction (reflection and transmission) and small-angle X-ray scattering were performed with nickel filtered Cu K_α radiation on locally constructed apparatus at Northwestern University. Compression molded, melt crystallized (MC) films with thickness about 0.5 mm were made from the same polymers and examined by the same methods.

3. Results

Densities are presented in Table 1, where it is apparent that the layered films are much more dense than the compression molded polymers. Phase fractions are evaluated with known phase densities, and the equilibrium weight fraction crystallinity w_c at room temperature is calculated from Flory theory. Of particular interest is observation that the crystalline fraction of layered HPB-39 is equal to the theoretical $w_c \approx 0.6$.

Similar changes are seen by DSC in Fig. 3; in addition to the heat of fusion being about 50% larger for HPB-20L, the final melting temperature T_m^f is 4 K higher than for the MC material. Apparent crystalline fractions from DSC in Table 2—estimated by comparing the heat of fusion ΔH_f to 296 J/g for crystalline polyethylene [12]—are lower than the density values in Table 1. The dashed curve for melting equilibrium copolymer crystals will be considered in Section 4.

The X-ray results show pronounced differences between the layer and melt crystallized copolymers as well. Figs. 4 and 5 present wide angle X-ray diffraction scans in reflection and transmission geometries, respectively. The peak intensity differences show that the (*hk*0) plane normals are preferentially in the plane of the multilayer film, hence the chain axis [00*l*] direction is concentrated near the layer normal. Additionally, the reflection patterns show a much smaller amorphous intensity for the layer sample, consistent with a decreased amorphous fraction. Amorphous intensity is not indicated properly in transmission (Fig. 5) because of the limited range of 2θ on the low angle side. Finally, SAXS patterns for the two preparations of HPB-20 are very different, as shown in Fig. 6. The pattern for the layer sample is much stronger with the X-ray beam in the film

Table 1
Density results

Polymer	ρ (kg/m^3)	v_c	w_c	Equil. w_c
HPB-20L	937	0.65	0.68	0.81
HPB-20MC	907	0.41	0.44	
HPB-39L	929	0.59	0.62	0.58
HPB-39MC	899	0.35	0.38	

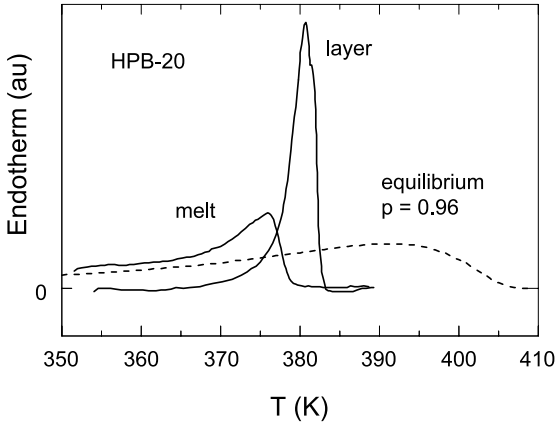

Fig. 3. DSC traces of the layer HPB-20 and the melt crystallized version of the same sample. The dashed line is calculated for melting of equilibrium crystals; it is the same as the corresponding curve in Fig. 2.

plane (perpendicular to the film normal), and intense arcs are seen in the direction of the layer normal. Hence the lamellar normals are preferentially in the layer normal direction, consistent with the WAXD results. Most striking is the drop in long period L from 14 to 8 nm when comparing melt crystallized and layer copolymers.

4. Discussion

Four related observations are of interest: The changes in melting temperature, crystalline fraction, lamellar morphology and texture that are induced by layer crystallization from solution. The final melting temperature is larger by 4 K in the layer samples. When analyzed with Eq. (2), l_f is seen to increase by 1 nm in Table 2. The most significant point is that the final melting temperature and corresponding maximum crystal thickness in these copolymers remain well below the values calculated from the Flory model, regardless of crystallization method. The reason for this

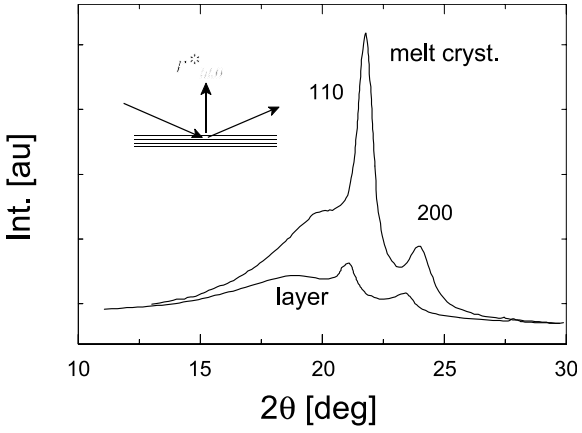

Fig. 4. Diffraction patterns in symmetric reflection (see inset) for layer and melt crystallized films. Weak 110 and 200 peaks for the layer sample indicate that r^*_{hk0} is preferentially in the plane of that film (see inset). Low amorphous intensity is consistent with a larger crystalline fraction.

Table 2
DSC results

Polymer	T_m^f (K)	l_f (nm)	Flory T_m^f (K)	Flory l_f (nm)	ΔH_f (J/g)	w_c^{DSC}
HPB-20L	382	8.1	407	64	114	0.39
HPB-20MC	378	7.1			73	0.25
HPB-39L	372	7.4	396	33	98	0.33
HPB-39MC	368	6.4			57	0.19

discrepancy is that extended sequence crystals with thickness $l \sim 30$–80 nm have extremely large secondary nucleation barriers [13], so thinner crystals are formed with folded sequences. This conclusion is reinforced by SAXS results considered below.

Crystallinity as estimated from density (Table 2) or heat of fusion (Table 3) is seen to increase by about 50% (relative) in the layer crystallized copolymers. There is little doubt that increased crystalline fraction comes from reduced impediments to sequences of appropriate lengths associating in the solution case. Melt crystallization of random copolymers is characterized by extensive frustration as evidenced by the insensitivity of crystallinity, long period, etc. to cooling rate, implying that sequence mobility remains limited over the times-seconds to hundreds of seconds—typically employed in crystallization. A logical explanation for this frustration is network formation by nucleation of individual chains in different crystals as sketched in Fig. 7(a). Winter and co-workers [14,15] have shown that a percolating network is formed in ethylene/α-olefin copolymers at a crystalline fraction below $w_c = 0.01$. Hence the majority of the crystallizable sequences are 'pinned' during cooling and have limited ability to diffuse or otherwise rearrange as required to solidify in a lattice. These impediments to mobility increase as the transformation proceeds. One can envision crystallization in this case being 'poisoned' by comonomer units and short sequences that are unable to vacate the growth front, thus preventing crystallizable sequences from participating in the transformation.

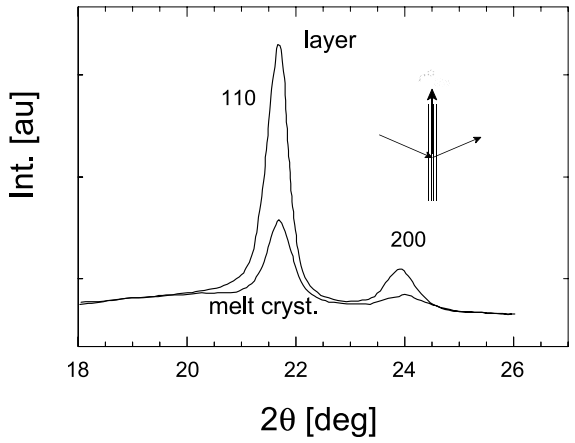

Fig. 5. Diffraction patterns in symmetric transmission (see inset) for the layer and melt crystallized films. Here the strong 110 and 200 peaks show directly that r^*_{hk0} is preferentially in the plane of the layered film.

Solidification from dilute solution is quite different. Most obvious is that multiple nucleation of individual chains is suppressed (network junctions are sparse) because of reduced polymer concentration; this condition is represented in Fig. 7(b). Also important is large segment mobility, even in the presence of a (loose) network, because non-reptative motion is feasible in the absence of entanglements that characterize the melt. Enhanced segment mobility mitigates the 'poisoning' that frustrates melt crystallization, and the observed crystalline fraction w_c is larger. Chain mobility is augmented appreciably even in very concentrated solutions where entanglements are presumably retained. This may result in the well-known phenomenon of solvent induced crystallization of a previously glassy polymer, a recent example of which is provided by Tashiro and Yoshioka [16].

Other published studies help clarify the crystallinity issue. Crist and Williams observed that melt crystallization achieves experimental w_c that approaches the equilibrium value when the amount of comonomer is great (e.g. 109 ethyl branches/1000 backbone C atoms or $p = 0.78$). The explanation for this is quite simple: the equilibrium crystallinity is low, e.g. 0.06, and multiple nucleation is rare because the fraction of crystallizable sequences is small. This dilution effect suppresses network formation, and the segment dynamics appear adequate, even in the entangled melt, to approach the (very small) equilibrium w_c.

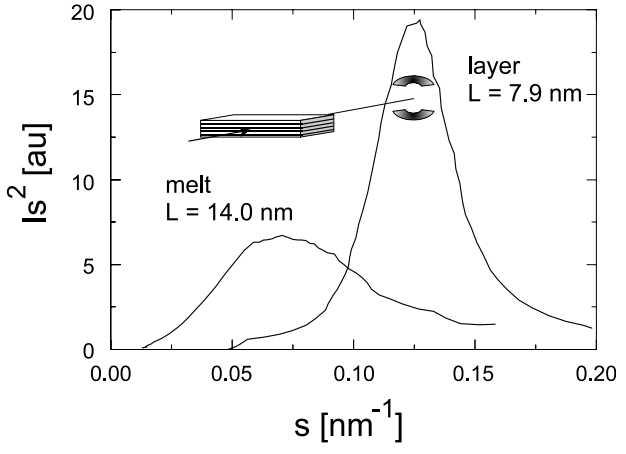

Fig. 6. Lorentz corrected SAXS patterns for layer and melt crystallized films. The pattern for the layer film was obtained with the X-rays incident in the film plane, as sketched. The pattern is a pair of well-defined arcs showing that lamellar normals are perpendicular to the plane of the layers. The pattern for the melt crystallized film is a continuous ring (isotropic array of lamellar normals).

Table 3
Estimates of phase thicknesses

Polymer	L (nm)	$l_c = v_c L$[a] (nm)	$l_a = (L - l_c)$ (nm)	l_f[b] (nm)
HPB-20L	7.9	5.1	2.8	8.1
HPB-20MC	14.0	5.7	8.3	7.1
HPB-39L	8.8	5.2	3.6	7.4
HPB-39MC	12.0	4.2	7.8	6.4

[a] From SAXS and density.
[b] From DSC (Table 2).

Gel crystallization of an ethylene–butene copolymer with 40 branches/1000 backbone C atoms (similar to HPB-39) was employed by Darras et al. [17]. In those experiments the solutions were 30–300 times more concentrated that the ones used here, and crystallization was induced by cooling rather than by combined cooling and evaporation. The important point is that the heat of fusion increased by about 50% as the solution concentration was lowered; crystallinity was enhanced by both a looser network and more solvent or swelling agent. More detailed comparisons are not warranted, as Darras' copolymer was compositionally heterogeneous (some chains with more comonomer than others). Domczy et al. [18] compared melt crystallized HBP's to those crystallized isothermally from dilute solution (ca. 0.1 g/L). They found that crystallinity w_c and (peak) melting temperature T_m were increased by solution crystallization by amounts similar to those observed here. No explanation was proffered for these changes, nor were comparisons made to equilibrium T_m^f or w_c.

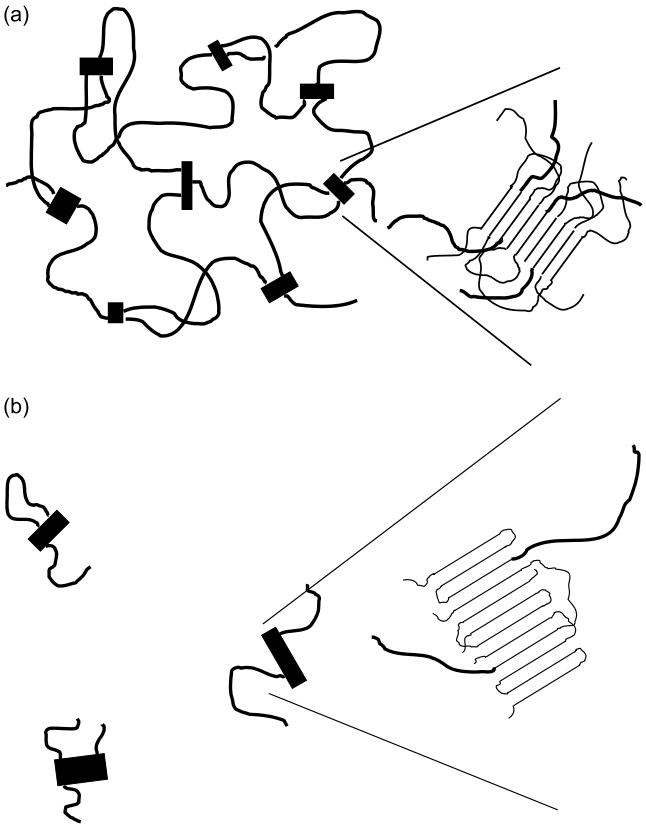

Fig. 7. (a) Sketch of network formation during early stages of crystallization of a random copolymer from the melt. The network strands for each folded sequence crystal are thick line. (b) Sketch of crystallization of a random copolymer from dilute solution. Multiple nucleation leading to a network is absent. More regular folding leads to a reduced thickness of the amorphous layers.

By combining the average long period L from SAXS with volume fraction crystallinity v_c from density, one obtains the estimates of crystal thickness l_c and amorphous layer thickness l_a in Table 3. While the identity period L decreases remarkably in the layer crystallized material (Fig. 6), the average crystal thickness l_c either decreases (HPB-20) or increases (HPB-39) by a moderate fraction. Note that the average l_c from SAXS and density is slightly less than the maximum l_f from DSC in all cases, the expected ranking that lends credence to these two estimates. Finally, the (average) amorphous thickness l_a is seen to decrease by more than 50% when each copolymer is crystallized from solution. The picture that emerges is that the crystals formed during precipitation from solution have roughly the same thickness as those in the melt crystallized copolymers. Intercrystalline amorphous layers, on the other hand, are 4–5 nm thinner in the solution crystallized samples, which accounts for the larger crystalline fraction w_c. Thinner amorphous layers likely reflect more regular folding of the crystals formed from solution. Domszy et al. previously noted without comment that the amorphous layer thickness was much reduced when the copolymer was crystallized from solution.

Pronounced uniaxial texture in the layer crystallized copolymers is the remaining observation to be considered. One might anticipate that the temperature and concentration gradients created during solvent evaporation would lead to growth of lamellar crystals in the layer normal direction. Should this be the case, [*uv*0] growth directions would be roughly parallel to the layer normal, while exactly the opposite is observed. There is ample evidence in the literature that polymer crystals grown from solution have preferred chain axis orientation along the surface normal of the resulting film. Storks was the first to report this sort of texture with crystals of *trans*-polyisoprene (gutta percha) in solution cast films about 20 nm thick [19]. Much thicker films (ca. 200 μm) formed by solvent evaporation from gel-crystallized ultra-high molecular weight polyethylene have chain axes similarly oriented [20,21]. In these cases the texture is ascribed to sedimentation and compression of the suspension of lamellar crystals as the solvent is removed to create a dry film. The same explanation was given by Darras et al. for gel crystallized films of an ethylene–butene copolymer. Gel crystallization is accomplished first by cooling the solution before shrinkage by solvent removal. In the present study the dilute solution is cooled with simultaneous solvent evaporation. From the crystalline texture we can infer that crystallization occurs quickly, and that the plate-like crystals sediment later as the solvent

is removed. This scenario supports the notion that chain segments (being in dilute solution) have high mobility during the crystallization process.

We close this discussion by considering the absolute values of crystallinity in Tables 1 and 2. The density derived values in Table 1 are from the simple two-phase model that employs measured $\rho_c = 980\ \mathrm{kg/m^3}$ for the crystalline regions And $\rho_a = 856\ \mathrm{kg/m^3}$ for the amorphous copolymer that are appropriate for the two copolymers used here. If the usual values of $\rho_c = 1000\ \mathrm{kg/m^3}$ and $\rho_a = 0.850\ \mathrm{kg/m^3}$ (correct for ethylene homopolymer) were used, w_c would drop from 0.62 to 0.56 for HBP-39L, which is still in the neighborhood of the equilibrium crystallinity of 0.58. The heat of fusion from DSC on the same layer material yields a weight fraction crystallinity $w_c^{DSC} = 0.33$, just over half the estimate from density. This sort of discrepancy is well known for random copolymers, and has been ascribed to inadequacies of the two-phase model. Mandlekern advocates an 'interphase' having a crystal-like density and an liquid-like enthalpy [22]. We believe that at least part of the difference lies in the apparent heat of fusion. First, ΔH_f is easily underestimated because the baseline is uncertain under the extensive low temperature tail of the melting region (Fig. 3). In addition, the heat of melting at low temperatures should be adjusted to account for decreased enthalpy of transition in thin crystals [23]. As neither of these refinements is employed here, it is likely that w_c^{DSC} is below the correct value. The density measurement, on the other hand is precise and unambiguous. We are confident that the crystalline fraction is reflected more reliably by density than by heat of fusion.

While the DSC traces at low temperatures are uncertain, the curves near the peak region are well defined. In Fig. 3 we have included equilibrium melting (derived from Fig. 2) to compare to experiment. Both melt and layer crystallized HPB-20 show a marked deficiency in thicker, highest melting crystals as described earlier. Furthermore, the amount of 'intermediate' crystals melting in the range of 375–380 K is larger than the equilibrium amount, because the longest sequences form folded sequence, not extended sequence, crystals. Although not shown, the curves for HPB-39 are comparable. If one accepts the density crystallinity $w_c \approx 0.6$ for this copolymer, then the folds associated with crystals do not add measurably to the non-crystalline fraction. Other interpretations are possible. Because the layer sample is crystallized from solution, the equilibrium w_c from Flory's melt crystallization theory may not be the appropriate limit, and the experimental value may be below that (unknown) theoretical crystallinity. Another possibility is that a small fraction of ethyl branches are included in the crystal [24], which would increase the equilibrium crystallinity, again by an unknown amount. And we do acknowledge that w_c from density may be subject to systematic error. Reliable theories and experiments to resolve these conjectures are not available at the present time.

5. Conclusions

Crystallization of random copolymers from solution yields a crystalline fraction w_c that is much higher than that achievable by melt crystallization. Enhanced crystallinity from solution undoubtedly derives from larger mobility that permits the crystallizable sequences between comonomer units to associate and crystallize. This mobility comes from the absence of a network (present in melt crystallization) and greater fluidity caused by the large solvent fraction.

Density estimates of crystallinity approach the theoretical prediction of Flory, especially for higher comonomer content where the restricting crystals are fewer. Quantitative estimates of phase thicknesses show that the amorphous regions in solution crystallized copolymers are much smaller than for melt crystallized material (about 3 vs. 8 nm). Furthermore, the experimental melting range is always appreciably below the theoretical one, because the thickest crystals are sequence (chain) folded, not extended sequence. Sequence folding is the consequence of classical kinetic nucleation barriers for thick crystals, an issue that is not overcome by dilution of the crystallizable chains. Uniaxial texture arises from sedimentation of the lamellar crystals during solvent evaporation. A unique feature of the layer crystallization scheme employed here is the film is formed without voids, etc. that characterize gel crystallized products.

Acknowledgements

This research was funded in part by the Gas Research Institute (Contract No. 5084-260-1051). The Office of Naval Research is acknowledged for a graduate fellowship awarded to T.M.F.

References

[1] Flory PJ. Trans Faraday Soc 1955;51:848–57.
[2] Crist B, Howard PR. Macromolecules 1999;32:3057–67.
[3] Kamal MS, Jeng L, Huang T. Can J Chem Eng 2002;80:432–42.
[4] Crist B. Polymer 2003;44:4563–72.
[5] Richardson MJ, Flory PJ, Jackson JB. Polymer 1963;4:221–36.
[6] Wunderlich B. J Chem Phys 1958;29:1395–404.
[7] Kilian HG. Thermochim Acta 1994;238:113–54.
[8] Crist B, Claudio ES. Macromolecules 1999;32:8945–51.
[9] Crist B, Williams DN. J Macromol Sci, Phys 2000;B39:1–13.
[10] Krigas TM, Carella JM, Struglinski MJ, Crist B, Graessley WW, Schilling FC. J Polym Sci, Polym Phys Ed 1985;23:509–20.
[11] Howard PR, Crist B. J Polym Sci, Part B: Polym Phys 1989;27:2269–82.
[12] Mandelkern L, Alamo G. Thermodynamic quantities governing melting. In: Mark JE, editor. Physical properties of polymers handbook. Woodbury, NY: AIP; 1996. p. 123.
[13] Hoffman JD, Davis GT, Lauritzen JI. The rate of crystallization of linear polymers with chain folding. In: Hannay NB, editor. Treatise on solid state chemistry, vol. 3. New York: Plenum Press; 1976 [chapter 7].

[14] Horst RH, Winter HH. Macromolecules 2000;33:130–6.
[15] Gelfer M, Horst RH, Winter HH, Heintz AM, Hsu SL. Polymer 2003; 44:2363–71.
[16] Tashiro K, Yoshioka A. Macromolecules 2002;35:410–4.
[17] Darras O, Seguela R, Rietch F. J Polym Sci, Part B: Polym Sci 1992; 30:349–59.
[18] Domszy RC, Alamo R, Mathieu PJM, Mandelkern L. J Polym Sci, Polym Phys Ed 1984;22:1727–44.
[19] Storks KH. J Am Chem Soc 1938;60:1753–61.
[20] Smith P, Lemstra PJ, Pijpers JPL, Kiel AM. Colloid Polym Sci 1981; 259:1070–80.
[21] Matsuo M, Manley RSJ. Macromolecules 1982;15:985–7.
[22] Alamo RG, Mandelkern L. Thermochim Acta 1994;238:155–201.
[23] Crist B, Mirabella F. J Polym Sci, Part B: Polym Sci 1999;37: 3131–40.
[24] Perez E, VanderHart DL, Crist B, Howard PR. Macromolecules 1987; 20:78–87.